# Progress towards colliding pulse injection

E. Esarey, C. B. Schroeder, and W. P. Leemans
*Lawrence Berkeley National Laboratory, University of California, Berkeley, California 94720*

Generation of ultrashort electron bunches by laser-triggered trapping of electrons in plasma-based accelerators is considered. Ultrashort, high-quality electron bunches can be produced in a controlled manner by the collision of laser pulses in an excited plasma wave. The basic theory of the colliding pulse injection mechanism is reviewed. Experimental progress towards electron beam production through colliding pulse injection is presented.

## I. INTRODUCTION

Perhaps the most basic and simplest form of a laser-plasma injector is the self-modulated regime of the laser wakefield accelerator (LWFA) [1, 2], in which a single laser pulse results in self-trapping and generation of a sub-ps electron bunch, however, with a large energy spread. Typically the self-trapped bunch is of high charge (up to 10 nC), with an energy distribution characterized by a Boltzmann distribution with temperature in the few MeV range. One possible mechanism for self-trapping is the direct wavebreaking of the plasma wakefield [3]. Since the phase velocity of the wakefield is near the speed of light, it is difficult to trap the background fluid electrons, which are undergoing the fluid oscillation that sustains the wakefield. The wake will trap the background electrons when the separatrix of the wake overlaps the plasma fluid orbit, which is the definition of wavebreaking. Wavebreaking of a cold one-dimensional (1D) plasma wave occurs at $E_{\rm WB} = [2(\gamma_p - 1)]^{1/2} E_0 \gg E_0$, where $v_p = c\beta_p = c(1 - \gamma_p^{-2})^{1/2}$ is the phase velocity of the plasma wave and $E_0 = cm_e\omega_p/e \simeq 96\left(n_0[\mathrm{cm}^{-3}]\right)^{1/2}$ V/m is the cold 1D nonrelativistic wavebreaking field, with $\omega_p = (4\pi n_0 e^2/m_e)^{1/2}$ the electron plasma frequency, $n_0$ the ambient electron density, $m_e$ and $e$ the electron rest mass and charge, respectively, and $c$ the speed of light in vacuum. Thermal and three-dimensional (3D) effects can lower this value, but typically wavebreaking requires nonlinear plasma waves with $E_z > E_0$. The observed wakefield amplitude, however, as measured in several experiments [4], appears to be in the range $E_z/E_0 \sim$10–30%, well below wavebreaking. This suggests that additional laser-plasma instabilities may play a role in lowering the effective wave breaking amplitude.

Alternatively, self-trapping and acceleration can result from the coupling of Raman backscatter (RBS) and Raman sidescatter (RSS) to the wakefield [5]. As the pump laser self-modulates, it also undergoes RBS, which is the fastest growing laser-plasma instability. RBS is observed in intense short pulse experiments, with reflectivities as high as 10–30% [4]. RBS generates red-shifted backward light of frequency $\omega_0 - \omega_p$ and wavenumber $-k_0$, which beats with the pump laser $(\omega_0, k_0)$ to drive a ponderomotive wave $(\omega_p, 2k_0)$. As the instability grows, the Raman backscatter beat wave, which has a slow phase velocity $v_p \simeq \omega_p/2k_0 \ll c$, can trap and heat background plasma electrons [6]. These electrons can gain sufficient energy and/or be displaced in phase by the beat wave such that they are trapped and accelerated to high energies in the wakefield. Simulations [5] indicate that coupling to RBS can lead to self-trapping at modest wakefield amplitudes, $E_z/E_0 \simeq 25\%$, much lower than the cold 1D threshold for direct wavebreaking. In 3D, this process can be enhanced by coupling to RSS.

When electrons become trapped in the fast wakefield, they become accelerated to high energies as they circulate inside the separatrix of the wake. A large energy spread for the trapped electrons results because (i) some fraction of the background electrons are continually being swept up and trapped in the wakefield as the laser pulse propagates into fresh plasma, and (ii) typically the self-guided propagation distance of the laser pulse is much greater than the detuning length for trapped electrons. This implies that deeply trapped electrons will circulate many revolutions within the separatrix, again resulting in a large energy spread.

For many applications, a small energy spread is desired. This can be achieved by using a standard LWFA (with $L \sim \lambda_p$, where $L$ is the laser pulse length and $\lambda_p = 2\pi c/\omega_p$ is the plasma wavelength), in which the wakefield is produced in a controlled manner at an amplitude below the wavebreaking or self-trapping threshold [1]. In principle, if a small energy spread electron bunch of duration small compared to $\lambda_p$ is injected into the wakefield at the proper phase, then the bunch can be accelerated while maintaining a small energy spread. This becomes problematic in the LWFA, since the wavelength of the accelerating field is small, e.g., $\lambda_p \simeq 30\,\mu$m for $n_0 \simeq 10^{18}\,\mathrm{cm}^{-3}$. Hence, a low energy spread requires an ultrashort bunch duration $\tau_b < \lambda_p/c$ that is injected at the optimal plasma wave phase with femtosecond timing accuracy. These requirements are beyond that of conventional electron beam injector technology (e.g., photoinjectors). On the other hand, the production of ultrashort laser pulses and the fs timing of multiple pulses is routine with compact chirped-pulse amplification (CPA) laser technology. As discussed in this section, ultrashort, high intensity laser pulses can be used to inject electrons into a single bucket (plasma wave period) of a standard LWFA [7–11].

Umstadter *et al.* [7] first proposed using an additional laser pulse to inject background plasma electrons into the

wake for acceleration to high energies. To generate ultrashort electron bunches with low energy spreads, the original laser injection method proposed by Umstadter *et al.* [7] utilizes two laser pulses which propagate perpendicular to one another. The first pulse (pump pulse) generates the wakefield via the standard LWFA mechanism, and the second pulse (injection pulse) intersects the wakefield some distance behind the pump pulse. The ponderomotive force $\vec{F} \simeq (m_e c^2/\gamma)\nabla a^2/2$ of the injection pulse can accelerate a fraction of the plasma electrons such that they become trapped in the wakefield. Here $a_0^2 \simeq 3.6 \times 10^{-19}(\lambda[\mu\mathrm{m}])^2 I[\mathrm{W/cm^2}]$, for a circularly polarized laser field, with $\lambda$ the laser wavelength and $I$ the laser intensity. Specifically, the axial (direction of propagation of the pump pulse along the $z$-axis) ponderomotive force of the injection pulse (propagating along the $x$-axis) scales as

$$F_z = \left(m_e c^2/\gamma\right)(\partial/\partial z)(a_1^2/2) \sim (m_e c^2/\gamma) a_1^2/r_1 \ , \quad (1)$$

where $a_1^2$ and $r_1$ are the normalized intensity and spot size of the injection pulse, respectively. A simple estimate for the change of momentum that an electron will experience due to the ponderomotive force of the injection pulse is $\Delta p_z \simeq F_z \tau_1 \sim (mc^2/\gamma) a_1^2 \tau_1 / r_1$, where $\tau_1$ is the injection pulse duration. It is possible for $\Delta p_z$ to be sufficiently large that electrons are injected into the separatrix of the wakefield such that they become trapped and accelerated to high energies. To inject into a single plasma wake bucket, it is necessary for both the injection pulse spot size and pulse length to be small compared to the plasma wavelength, i.e., $r_1^2 \ll \lambda_p^2$ and $c^2\tau_1^2 \ll \lambda_p^2$. Simulations [7], which were performed for ultrashort pulses at high densities ($\lambda_p/\lambda = 10$ and $E_z/E_0 = 0.7$), indicated the production of a 10 fs, 21 MeV electron bunch with a 6% energy spread. However, high intensities ($I > 10^{18}\,\mathrm{W/cm^2}$) are required in both the pump and injection pulses ($a_0 \simeq a_1 \simeq 2$).

Simulations by Hemker *et al.* [9] point out that additional electron injection into one or more wake buckets can result due to influence of the wake associated with the injection pulse, which can be significant due to the high intensity of the injection pulse ($a_1 \gtrsim 1$). Umstadter *et al.* [7] also discuss the possibility of injection using an injection pulse that propagates parallel, but some distance behind, the pump pulse. The injection pulse would have a tighter focus (and hence smaller Rayleigh length) than the pump pulse, and would be phased appropriately such that it locally drives the wakefield to an amplitude that exceeds wavebreaking, thus resulting in local trapping of electrons.

Esarey *et al.* [8] proposed and analyzed the colliding pulse injection method that relies on the beat wave produced by the collision of two counterpropagating laser pulses. Beat wave injection differs intrinsically from the method of ponderomotive injection discussed above in that the source and form of the ponderomotive force differs in these two methods. In ponderomotive injection, injection is the result of the ponderomotive force associated with the *envelope* (time-averaged intensity profile) of a single pulse. In beat wave injection, injection is the result of the ponderomotive force associated with the *slow beat wave* of two intersecting pulses.

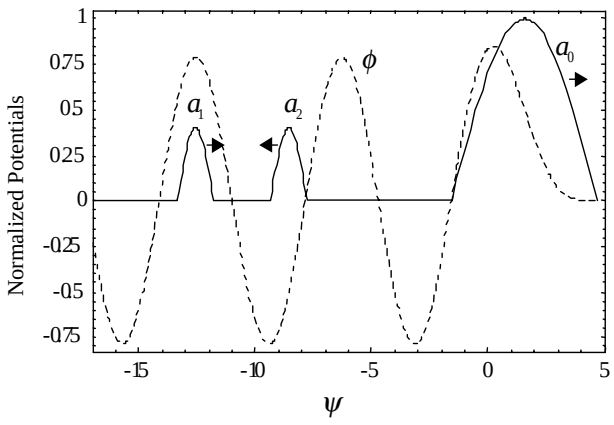


FIG. 1: Profiles of the pump laser pulse $a_0$, the wake $\phi$ (*dashed line*), and the forward $a_1$ injection pulse, all of which are stationary in the $\psi = k_p(z - v_p t)$ frame, and the backward injection pulse $a_2$, which moves to the left at $\simeq 2c$.

## II. COLLIDING PULSE INJECTION

Colliding pulse injection [8, 10, 11] uses three short laser pulses: an intense ($a_0^2 \simeq 1$) pump pulse (denoted by subscript 0) for plasma wake generation, a forward going injection pulse (subscript 1), and a backward going injection pulse (subscript 2), as shown in Fig. 1. The frequency, wavenumber, and normalized intensity are denoted by $\omega_i$, $k_i$, and $a_i$ ($i = 0, 1, 2$). Furthermore, it is assumed that $k_1 \simeq k_0$, $k_2 \simeq -k_0$, and $\omega_1 - \omega_2 = \Delta\omega \gg \omega_p$. The pump pulse generates a plasma wake with phase velocity near the speed of light ($v_{p0} \simeq c$). The forward injection pulse travels at a fixed distance behind the pump pulse, which determines the position (i.e., phase) of the injected electrons. The injection pulses are orthogonally polarized to the pump laser pulse, such that the pump pulse and backward going injection pulse do not beat. When the injection pulses collide some distance behind the pump, they generate a slow ponderomotive beat wave of the form $a_1 a_2 \cos(\Delta k z - \Delta\omega t)$ (here $\Delta k = k_1 - k_2 \simeq 2k_0$) with a phase velocity $v_{pb} \simeq |\Delta\omega|/2k_0 \ll c$. The axial force associated with this beat wave scales as

$$\begin{aligned} F_z &= (m_e c^2/\gamma)(\partial/\partial z) a_1 a_2 \cos(2k_0 z - \Delta\omega t) \\ &\sim (m_e c^2/\gamma) 2k_0 a_1 a_2 \ . \end{aligned} \quad (2)$$

During the time in which the two injection pulses overlap, a two-stage acceleration process can occur, i.e., the slow beat traps and heats background plasma electrons which, as a result of shifts in their momentum and phase, can be injected into the fast wakefield for acceleration to high energies. The ratio of the axial force of the beat wave

to that of a single pulse in the ponderomotive injection scheme scales as

$$\frac{F_{z,\mathrm{beat}}}{F_{z,\mathrm{pond}}} \sim \frac{2k_0 a_1 a_2}{a_p^2/r_p} \ , \tag{3}$$

where the subscript $p$ refers to the single ponderomotive injection pulse and the contribution of the relativistic factor $\gamma$ (which is different for the two cases) is neglected. For comparable injection pulse intensities ($a_1 \simeq a_2 \simeq a_p$), the ratio scales as $4\pi r_p/\lambda_0 \gg 1$, i.e., the axial force of the beat wave is much greater than the ponderomotive force of a single pulse. Consequently, colliding pulses can result in electron injection at relatively low intensities ($a_1 \sim a_2 \sim 0.2$), as well as at relatively low densities ($\lambda_p/\lambda \sim 100$), thus allowing for high single-stage energy gains. Furthermore, the colliding pulse concept offers detailed control of the injection process: the injection phase can be controlled via the position of the forward injection pulse, the beat phase velocity via $\Delta\omega$, the injection energy via the pulse amplitudes, and the injection time (number of trapped electrons) via the backward pulse duration.

To help understand the injection mechanism, it is insightful to consider the electron motion in the wakefield and in the colliding laser fields individually. In the absence of the injection pulses, electron motion in a 1D wakefield is described by the Hamiltonian $H_w = \gamma - \beta_p(\gamma^2-1)^{1/2} - \phi(\psi)$, where $\phi = \phi_0 \cos\psi$, $v_p = c\beta_p$ is the phase velocity of the plasma wave, $\gamma_p = (1-\beta_p^2)^{-1/2}$, and $\psi = k_p(z - v_p t)$. The electron orbits in phase space $(u_z, \psi)$ are given by $H_w(u_z,\psi) = H_0$, where $H_0$ is a constant, $\gamma^2 = 1 + u_z^2$, and $u_z = \gamma\beta_z$ is the normalized axial momentum, which is given by

$$u_z = \beta_p\gamma_p^2\left[H_0 + \phi(\psi)\right] \pm \gamma_p\left\{\left[\gamma_p^2\left[H_0+\phi(\psi)\right]^2 - 1\right\}^{1/2} \ . \tag{4}$$

The 1D separatrix (the boundary between trapped and untrapped orbits) is given by $H_w(\beta_z,\psi) = H_w(\beta_p,\pi)$, i.e., $H_0 = H_{1\mathrm{D}} = 1/\gamma_p - \phi(\pi)$. The maximum and minimum electron momentum on the 1D separatrix occur at $\psi = 0$ and are (in the limits $2\phi_0\gamma_p \gg 1$ and $\gamma_p \gg 1$) $u_{w,\max} \simeq 4\gamma_p^2\phi_0$ and $u_{w,\min} \simeq 1/4\phi_0 - \phi_0$.

The 1D theory neglects the effects of transverse focusing. Associated with a 3D wake is a periodic radial field which is $\pi/2$ out of phase with accelerating field, i.e., there exists a phase region of $\lambda_p/4$ for which the wake is both accelerating and focusing (as opposed to the $\lambda_p/2$ accelerating region in 1D). If an electron is to remain in this phase region, it must lie within the "3D separatrix" defined by $H_w(\beta_z,\psi) = H_w(\beta_p,\pi/2)$, i.e., Eq. (4) with $H_0 = H_{3\mathrm{D}} = 1/\gamma_p - \phi(\pi/2)$. The extremum on the 3D separatrix are given by $u_{w,\max} \simeq 2\gamma_p^2\phi_0$ and $u_{w,\min} \simeq 1/2\phi_0 - \phi_0/2$. This value of $u_{w,\max} \simeq 2\gamma_p^2\phi_0$ gives the usual maximum energy gain due to linear dephasing in a 3D wake.

The background plasma electrons lie on an untrapped orbit (below the separatrix) $u_{zf}$ given by $H_w(u_{zf},\psi) = 1$, i.e., Eq. (4) with $H_0 = 1$. At wavebreaking, the bottom of the separatrix $u_{w,\min}$ coalesces with the plasma fluid orbit, $u_{zf} = u_{w,\min}$. This occurs at the well-known wavebreaking field of $E_{\mathrm{WB}}/E_0 = [2(\gamma_p - 1)]^{1/2}$.

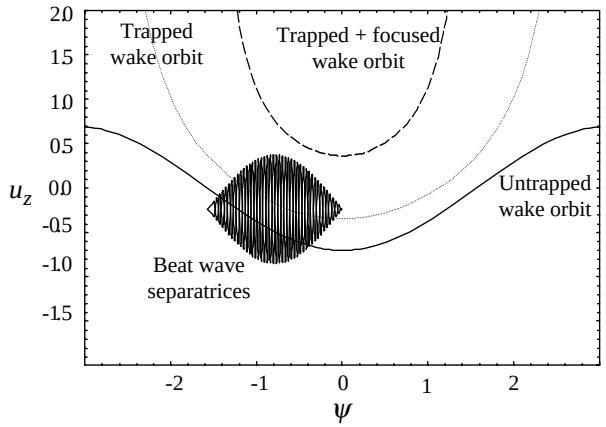


FIG. 2: Longitudinal phase space $(\psi, u_z)$ showing beat wave separatrices, an untrapped plasma wave orbit (*solid line*), a trapped plasma wave orbit (*dotted line*), and a trapped and focused plasma wave orbit (*dashed line*).

Consider the motion of electrons in the colliding laser fields in the absence of the wakefield. The beat wave leads to formation of phase space buckets (separatrices) of width $2\pi/\Delta k \simeq \lambda_0/2$, which are much shorter than those of the wakefield ($\lambda_p$). In the colliding laser fields, the electron motion is described by the Hamiltonian $H_b = \gamma - \beta_b[\gamma^2 - \gamma_\perp^2(\psi_b)]^{1/2}$, where the space charge potential is neglected. Circular polarization is assumed such that $\gamma_\perp^2 = 1 + a_0^2 + a_1^2 + 2a_0a_1\cos\psi_b$, where $\psi_b = (k_1 - k_2)(z - v_b t)$ and $v_b = c\beta_b = \Delta\omega/(k_1 - k_2) \simeq \Delta\omega/2k_0$ is the beat phase velocity, assuming $\omega_p^2/\omega_0^2 \ll 1$. The beat separatrix is given by $H_b(\beta_z,\psi_b) = H_b(\beta_b, 0)$ with a maximum and minimum axial momenta of

$$u_{b,m} = \gamma_b\beta_b\left[1 + (a_0 + a_1)^2\right]^{1/2} \pm 2\gamma_b(a_0a_1)^{1/2} \ . \tag{5}$$

An estimate for the threshold for injection into the wakefield can be obtained by a simple phase-space island overlap criteria. This is done by considering the effects of the wakefield and the beat wave individually, as done above, and by requiring that the beat wave separatrix overlap both the wakefield separatrix and the plasma fluid oscillation (illustrated in Fig. 2): (i) the maximum momentum of the beat wave separatrix $u_{b,\max}$ exceed the minimum momentum of the wakefield separatrix $u_{w,\min}$, i.e., $u_{b,\max} \geq u_{w,\min}$, and (ii) the minimum momentum of the beat wave separatrix $u_{b,\min}$ be less than the plasma electron fluid momentum $u_{zf}$, i.e., $u_{b,\min} \leq u_{zf}$. Conditions (i) and (ii) imply a beat wave threshold

$$(a_1a_2)_{\mathrm{th}}^{1/2} = \frac{(1 - H_0)}{4\gamma_b(\beta_p - \beta_b)} \ , \tag{6}$$

and an optimal wake phase for injection (location of the

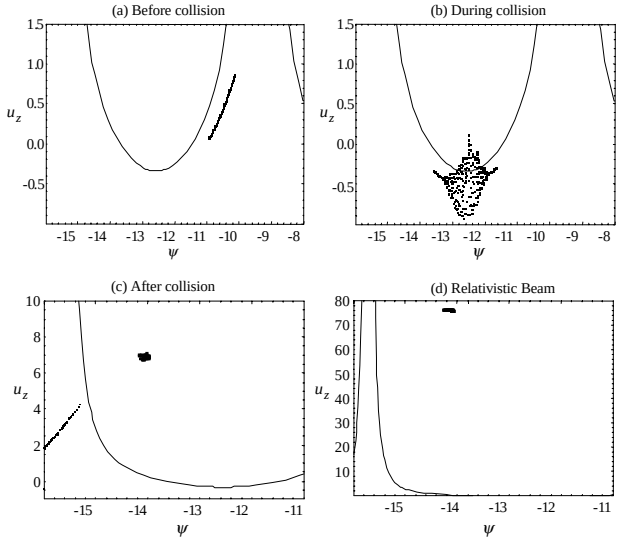


FIG. 3: Electron distribution in longitudinal $(u_z, \psi)$ phase space (**a**) before injection pulse collision ($\omega_p \Delta t = 0$), (**b**) during collision ($\omega_p \Delta t = 3$), (**c**) just after collision ($\omega_p \Delta t = 14$), and (**d**) at $\omega_p \Delta t = 114$ (38 MeV electron bunch with 1 fs duration, 0.2% energy spread, and 0.9 mm-mrad normalized emittance). The separatrix between trapped and untrapped wake orbits (*solid line*) is shown.

forward injection pulse)

$$\cos\psi_{\rm opt} = \phi_0^{-1}\left[(1-\beta_b\beta_p)\gamma_b\gamma_\perp(0) - (1+H_0)/2\right] \ , \quad (7)$$

where $H_0 = H_{\rm 1D} = 1/\gamma_p + \phi_0$ for the 1D wake separatrix and $H_0 = H_{\rm 3D} = 1/\gamma_p$ for the 3D wake separatrix (trapped and focused). In the limits $\gamma_p^2 \gg 1$, $\beta_b^2 \ll 1$, and $a_i^2 \ll 1$, Eqs. (6) and (7) become $4(a_1 a_2)_{\rm th}^{1/2} \simeq (1-H_0)(1+\beta_b)$ and $2\phi_0 \cos\psi_{\rm opt} \simeq 1 - H_0 - 2\beta_b$ with $H_{\rm 1D} \simeq \phi_0$ and $H_{\rm 3D} \simeq 0$. As an example, $\phi_0 = 0.7$, $\beta_b = -0.02$, and $\gamma_p = 50$ imply a threshold of $(a_1 a_2)_{\rm th}^{1/2} \simeq 0.25$ and an optimal injection phase of $\psi_{\rm opt} \simeq 0$ for injection onto a trapped and focused orbit.

To further evaluate the colliding laser injection method, the motion of test particles in the combined wake and laser fields was simulated in 3D [10]. In the numerical studies, the laser pulse axial profiles were half-period sine waves (linearly polarized with Gaussian radial profiles) with peak amplitude $\sqrt{2}a_i$, such that $\langle a^2 \rangle = a_i^2$, and length $L_i$. The wakefield is assumed to be nonzero for $\psi \leq 3\pi/4$ (see Fig. 1) and the test particles are loaded uniformly with $\psi > 3\pi/4$ (initially at rest).

An example of the injection process is given in Fig. 3, which shows the evolution in longitudinal phase space $(u_z, \psi)$ of the test electron distribution (a) before the collision of the injection laser pulses (in the untrapped fluid orbit of the wake) at $\omega_p t = 36$, (b) during the collision (crossing the wake separatrix) at $\omega_p t = 39$, (c) after the collision at $\omega_p t = 50$, and (d) the resulting energetic electron bunch at $\omega_p t = 150$ ($z = 0.7$ mm). Also shown is the 1D wake separatrix. The parameters

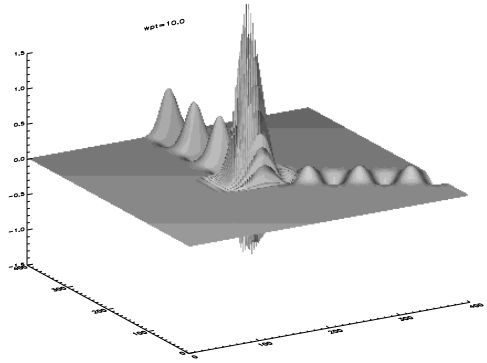

FIG. 4: Electric field profiles and corresponding wakefields, plotted during the collision of the drive pulse and colliding pulse versus $x$ and $z - ct$ (where $z$ is the drive pulse propagation direction), for the two-pulse configuration with a 30° interaction geometry.

are $a_1 = a_2 = 0.32$, $L_0 = 4L_1 = 4L_2 = \lambda_p = 40\,\mu$m, $\phi_0 = 0.7$, $\lambda_0 = \lambda_2 = 0.8\,\mu$m, $\lambda_1 = 0.83\,\mu$m, and $r_0 = r_1 = r_2 = 15\,\mu$m, with the position of the forward injection pulse centered at $\psi_{\rm inj} = -12.6$. After $z \simeq 0.7$ mm of propagation following the collision, Fig. 3(d), the bunch length is 1 fs with a mean energy of 38 MeV, a fractional energy spread of 0.2%, and a normalized transverse emittance of 0.9 mm-mrad. The trapping fraction $f_{\rm trap}$ is 3%, corresponding to $2.6 \times 10^6$ bunch electrons. Here, $f_{\rm trap}$ is defined as the fraction of electrons trapped that were initially loaded in a region of length $\lambda_p/4$ with $r \leq 2\,\mu$m (simulations indicate that electrons loaded outside this region are not trapped). Note that the bunch number can be increased by increasing the laser spot sizes (i.e., laser powers). For example, when the laser spot sizes are doubled $r_i = 30\,\mu$m in the simulation of Fig. 3 (all other parameters as in Fig. 3), the number of trapped electrons increases to $1.5 \times 10^7$ and the normalized transverse emittance increases to 3.9 mm-mrad. Estimates indicate that space charge effects can be neglected while the bunch remains inside the plasma [10].

## III. COLLIDING PULSE INJECTION EXPERIMENTS

Experiments on laser injection methods are being pursued at several laboratories world-wide. For example, at Lawrence Berkeley National Laboratory (LBNL), experiments are underway on the colliding pulse method. The initial set of experiments uses only two pulses: a pump pulse for wakefield generation and a single backward propagating injection pulse (see Fig. 4). Here the pump and injection pulses have the same polarization such that injection results from the slow ponderomotive beat wave that is produced when the injection pulse collides with the tail of the pump pulse. Experimentally, the use of collinear pulses is technically challenging as

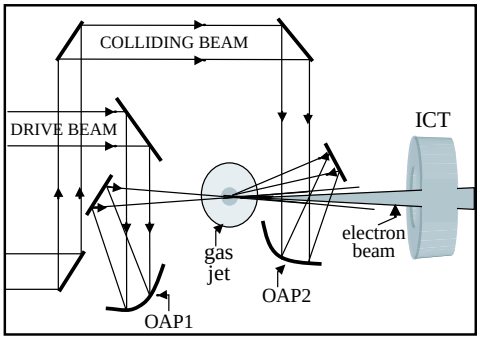


FIG. 5: Lay-out of experiment showing the drive and colliding laser beams exiting the compressor. The drive (colliding) beam is focused onto the off-axis parabola OAP1 (OAP2), which focus the beams under a 30° angle onto the gas jet. The resulting electron beam charge is measured using the integrating current transformer (ICT).

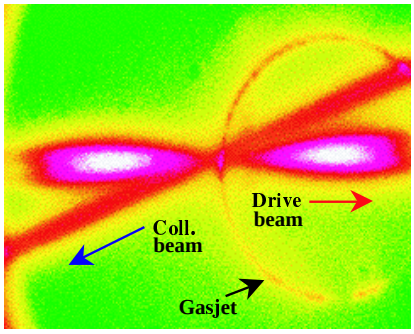


FIG. 6: Top view CCD camera image of the plasmas produced by two laser pulses propagating in a backfilled chamber indicating the spatial overlap of the beams: drive beam (horizontal) and colliding beam (30°). The measured light emission is from recombination in the Helium plasma, and the shape follows the Gaussian iso-intensity contours of a focused laser beam. The drive beam was focused at the upstream edge of the gas jet with a smaller f-number lens than the colliding beam and hence has a shorter Rayleigh length. Ring passing through the intersection point is caused by laser light scattering off the gas jet edge.

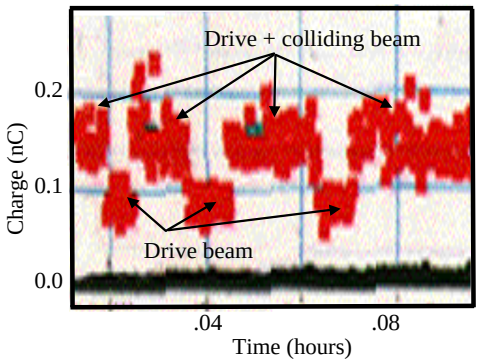


FIG. 7: Electron beam charge measured using the ICT versus clock time when a single drive beam is used (lower charge level) and when both drive and colliding beams are used (higher level).

the counterpropagating pulse must be reflected by a mirror through which the electron beam must propagate and off which the high power drive pulse must be reflected. Ultra-thin, dielectrically coated substrates are being developed, but substrates that can handle the high fluence in these experiments are not presently commercially available. Therefore the current experimental implementation uses non-collinear injection of the the drive and colliding beams. Non-collinear injection has been explored theoretically and shown to provide nearly the same beam quality as collinear injection [12].

In these experiments two intense short laser pulses were produced by a 10 Hz, Ti:$Al_2O_3$, CPA laser system [13]. Low energy pulses ($\lambda \simeq 0.8\,\mu$m) from a laser oscillator were first temporally stretched, amplified to 1 mJ using a regenerative amplifier, split into two pulses, and then amplified to 1 J/pulse and 0.3 J/pulse, respectively. Each pulse was then compressed using its own grating based optical compressor (installed in a vacuum chamber) to pulse widths as short as 45 fs with an overall power transmission efficiency of about 50% onto a gas jet target.

Following compression, the main drive laser beam was focused to a 6 $\mu$m spot size with a 30 cm focal length (F/4) off-axis parabola (OAP) onto the pulsed gas jet. With this single drive beam, electron bunches have been produced through self-modulation containing up to 5 nC charge with electron energy in excess of 40 MeV [2]. The colliding beam was focused to a 8 $\mu$m spot size with an identical OAP onto the pulsed gas jet with a 30 degree angle with respect to the drive beam. The lay-out of the experiment is shown in Fig. 5. The intersection of the beams was measured using a CCD camera looking from above onto the plasma region and with side-on imaging. The top-view CCD camera image is shown in Fig. 6, indicating the spatial overlap of the colliding and drive beams.

The total charge per bunch and spatial profile of the electron beam were measured using an integrating current transformer (ICT) and phosphor screen imaged onto a 16 bit CCD camera, respectively. As shown in Fig. 7, preliminary results have been obtained that indicate electron yields have been affected by the second laser beam which intersected the forward going drive laser beam at 30 degrees. Note that the peak power in the drive beam was lowered to reduce the charge production to about 0.1 nC. The charge enhancement resulting from the second pulse could be due to several mechanisms, such as generation of a beat wave (i.e., colliding pulse injection), heating of the background electrons, or other stochastic processes. Ongoing experiments at LBNL are in the process of measuring the electron beam spectra and carrying out various parametric studies to understand in detail the underlying injection mechanisms.

**Acknowledgments**

This work was supported by the U.S. Department of Energy under Contract No. DE-AC03-76SF0098.

[1] E. Esarey, P. Sprangle, J. Krall, and A. Ting, IEEE Trans. Plasma Sci. **24**, 252 (1996).
[2] W. P. Leemans, P. Catravas, E. Esarey, C. G. R. Geddes, C. Toth, R. Trines, C. B. Schroeder, B. A. Shadwick, J. van Tilborg, and J. Faure, Phys. Rev. Lett. **89**, 174802 (2002).
[3] D. Gordon, K.-C. Tzeng, C. E. Clayton, A. E. Dangor, V. Malka, K. A. Marsh, A. Modena, W. B. Mori, P. Muggli, Z. Najmudin, et al., Phys. Rev. Lett. **80**, 2133 (1998).
[4] C. I. Moore, A. Ting, K. Krushelnick, E. Esarey, R. F. Hubbard, B. Hafizi, H. R. Burris, C. Manka, and P. Sprangle, Phys. Rev. Lett. **79**, 3909 (1997).
[5] E. Esarey, B. Hafizi, R. Hubbard, and A. Ting, Phys. Rev. Lett. **80**, 5552 (1998).
[6] P. Bertrand, A. Ghizzo, S. J. Karttunen, T. J. H. Pattikangas, R. R. E. Salomaa, and M. Shoucri, Phys. Plasmas **2**, 3115 (1995).
[7] D. Umstadter, J. K. Kim, and E. Dodd, Phys. Rev. Lett. **76**, 2073 (1996).
[8] E. Esarey, R. F. Hubbard, W. P. Leemans, A. Ting, and P. Sprangle, Phys. Rev. Lett. **79**, 2682 (1997).
[9] R. G. Hemker, K.-C. Tzeng, W. B. Mori, C. E. Clayton, and T. Katsouleas, Phys. Rev. E **57**, 5920 (1998).
[10] C. B. Schroeder, P. B. Lee, J. S. Wurtele, E. Esarey, and W. P. Leemans, Phys. Rev. E **59**, 6037 (1999).
[11] E. Esarey, C. B. Schroeder, W. P. Leemans, and B. Hafizi, Phys. Plasmas **6**, 2262 (1999).
[12] G. Fubiani, E. Esarey, C. B. Schroeder, and W. P. Leemans (2003), in preparation.
[13] W. P. Leemans, D. Rodgers, P. E. Catravas, C. G. R. Geddes, G. Fubiani, E. Esarey, B. A. Shadwick, R. Donahue, and A. Smith, Phys. Plasmas **8**, 2510 (2001).